ADVANCED MATERIALS
www.advmat.de

Toward Superior Capacitive Energy Storage: Recent Advances in Pore Engineering for Dense Electrodes

Congcong Liu, Xiaojun Yan, Fei Hu, Guohua Gao, Guangming Wu, and Xiaowei Yang**

With the rapid development of mobile electronics and electric vehicles, future electrochemical capacitors (ECs) need to store as much energy as possible in a rather limited space. As the core component of ECs, dense electrodes that have a high volumetric energy density and superior rate capability are the key to achieving improved energy storage. Here, the significance of and recent progress in the high volumetric performance of dense electrodes are presented. Furthermore, dense yet porous electrodes, as the critical precondition for realizing superior electrochemical capacitive energy, have become a scientific challenge and an attractive research focus. From a pore-engineering perspective, insight into the guidelines of engineering the pore size, connectivity, and wettability is provided to design dense electrodes with different porous architectures toward high-performance capacitive energy storage. The current challenges and future opportunities toward dense electrodes are discussed and include the construction of an orderly porous structure with an appropriate gradient, the coupling of pore sizes with the solvated cations and anions, and the design of coupled pores with diverse electrolyte ions.

1. Introduction

Electrochemical energy storage (EES) has attracted tremendous attention because it is believed to be one of the most promising solutions in storing and delivering electricity for the rapid development of mobile electronics and electric vehicles.[1–4] Among various EES devices, electrochemical capacitors (ECs, also called supercapacitors) have become a hot topic of research due to their remarkable features, such as their fast charging capabilities, long cycle lifetime, superior stability, and safe operation.[5–9] Some previous studies have mainly focused on improving the gravimetric capacitive performance of the electrode materials but with a low packing density, which has led to excessive pores/channels in the electrode that are flooded by the electrolyte, thereby increasing the weight of the device without adding capacitance.[10] In this respect, compared with the gravimetric performance, the energy and power densities per volume of the device or electrode may provide a realistic indication of the performance. Currently, the volumetric energy density of commercially available ECs is ≈5–8 Wh L^{-1}, which is considerably lower than those of lead-acid batteries (50–90 Wh L^{-1}).[11,12] Therefore, the design and development of advanced EC electrodes with high volumetric performance to satisfy the requirement for future practical applications remains a great challenge for materials scientists.

EC devices include two electrodes, an electrolyte, a separator, current collectors, and a cell case. For the key electrode component, a high volumetric energy and power density is indicative of more active material per unit volume of the device and meanwhile achieving great energy storage performance and high charge/discharge characteristics.[10] Since the energy-storage mechanism of the double layer capacitive behavior relies on the electrode/electrolyte interface and the electrolyte-ion transport in porous channels, the surface and pore structures of the dense electrode must precisely couple with the fluid electrolyte while simultaneously optimizing numerous resulting interfaces.[13] Thus, superior electrodes should possess a large ion-accessible interface, good electrical conductivity, chemical stability in different electrolytes, a relatively high packing density, and especially porous structures favorable toward electrolyte-ion transport.

In the past decade, several significant accomplishments on the volumetric performance have been demonstrated based mainly on carbon materials, such as activated carbons (ACs),[14,15] carbide-derived carbons (CDCs),[16] single-walled carbon nanotubes (SWNTs),[17] porous carbon,[18] and recently emerging graphene[19–23] and their composites because of their large specific surface area (SSA), high electrical conductivity, and tunable density/porosity. Recently, new 2D materials, such as MXenes and metallic 1T phase transition-metal dichalcogenides (TMDs), have also indicated their potential in volumetric energy storage systems due to their higher density and electrical conductivity.[24–27] Even though some research progress has been reported to improve the volumetric performance of

C. Liu, X. Yan, Prof. F. Hu, Prof. G. Wu, Prof. X. Yang
Interdisciplinary Materials Research Center
Key Laboratory of Advanced Civil Engineering Materials (Ministry of Education)
School of Materials Science and Engineering
Tongji University
Shanghai 201804, China
E-mail: wugm@tongji.edu.cn; yangxw@tongji.edu.cn
Dr. G. Gao, Prof. G. Wu
Shanghai Key Laboratory of Special Artificial Microstructure Materials and Technology
School of Physics Science and Engineering
Tongji University
Shanghai 200333, China
The ORCID identification number(s) for the author(s) of this article can be found under https://doi.org/10.1002/adma.201705713.

DOI: 10.1002/adma.201705713

electrode, a clear understanding of the dense electrodes with appropriate nanoporous structures coupled well with the electrolyte ions is still lacking.

Here, we provide a summary of the significant research breakthroughs in the superior volumetric performance of dense electrodes made from a range of nanoporous materials. Moreover, this review will focus primarily on the engineering of pores to design a dense yet porous electrode with excellent volumetric performance. Finally, the current challenges, future directions, and future opportunities are briefly discussed.

2. The Significant Influence of the Electrode Density on the Volumetric Performance

The efficiency of the electrode could be determined by its volumetric energy density ($E_{\text{vol-stack}}$)

$$C_{\text{vol}} = C_{\text{wt-C}} \times \rho \tag{1}$$

$$E_{\text{vol-electrode}} = \frac{C_{\text{vol}} \times U^2}{8} \tag{2}$$

$$E_{\text{vol-stack}} = E_{\text{vol-electrode}} \times f_{\text{electrode}} \tag{3}$$

where $E_{\text{vol-stack}}$ relates to the gravimetric capacitance of a single electrode $C_{\text{wt-C}}$, the packing density of active materials in the electrode (ρ), the volume fraction of the electrodes in the device stack ($f_{\text{electrode}}$), as well as the nominal voltage (U) of the ECs.[19] Obviously, the electrode density is a non-negligible factor deciding the final volumetric performance. A highly porous structure for a high $C_{\text{wt-C}}$ together with a high packing density may yield a superior volumetric capacitance, in which the intrinsic density/porosity and processing method of the active materials are essential.

ACs as the electrode materials have a history of use in ECs due to their moderate cost, large SSA (900–3500 $m^2\ g^{-1}$), and specific capacitance in the range of 50–80 F cm^{-3}.[28] However, the relatively low density (<0.5 g cm^{-3}) and fixed pore structures of most ACs may not function well in applications for volumetric capacitive energy storage. To increase the density of AC electrodes, a low-porosity carbonaceous material was synthesized by the one-step carbonization of an oxygen-rich biopolymer, resulting in a high density of 0.9 g cm^{-3} and a volumetric capacitance of 180 F cm^{-3} in 1.0 M H_2SO_4 electrolyte.[29]

Porous carbons are also considered as candidates for ECs due to their large surface area, controlled uniform pore structure, and relatively high conductivity.[30,31] Different methods were explored to synthesize porous carbons electrode with high density by regulating the preparation process.[32,33] Dense porous carbon (0.93 g cm^{-3}) was prepared through direct thermolysis of the metal–organic framework with carbon tetrachloride and ethylenediamine as the additional carbon sources, which revealed a volumetric capacitance of 252 F cm^{-3} in aqueous electrolyte (6 M KOH).[34] In addition, a higher density of 1.32 g cm^{-3} for the porous carbon electrode has been reported by collapsing the hierarchical carbon nanocage (CNC) materials via capillarity, showing a high volumetric capacitance of 233 F cm^{-3} at 1 A g^{-1} in the neat $EMIMBF_4$ electrolyte.[35] CDC is a kind of porous carbon produced by selectively etching metals from metal carbides. It has shown promise as a high volumetric capacitive electrode owing to its fine-tuned density from 0.53–0.73 g cm^{-3} by controlling the starting precursors and the chlorination conditions.[36–38] A volumetric capacitance of 160–180 F cm^{-3} was reported by Gogotsi's group.[36]

SWNTs have demonstrated attractive potential with respect to EC applications because of their unique porous structure and excellent electrical conductivity.[39–41] However, as an active material, their relatively low density (0.3 g cm^{-3}) is unfavorable for compact capacitive energy storage. Thus, various approaches have been devoted toward creating a densely packed SWNT electrode. As an example, Hata's group prepared an aligned high densely packed SWNT material (0.57 g cm^{-3}) by using the zipping effect of liquids to draw the nanotubes together (**Figure 1**).[42] The packing density of SWNT electrode can still be increased to 0.83 g cm^{-3} by using a layer-by-layer technique, which yielded volumetric capacitances of 132 F cm^{-3} within aqueous electrolytes.[43] These dense SWNT films demonstrated great potential in the volumetric capacitive energy storage field.

Guangming Wu received his Ph.D. degree from Tongji University in 1996. He was promoted to professor of physics in 2002 at Tongji University, and now is the director of the Key Laboratory of Advanced Civil Engineering Materials, Ministry of Education. His current research interests include synthesis and interfacial modification of 2D oxide and sulfide-based nanomaterials and 3D functional porous materials, and applications in energy storage, energy saving buildings, and smart windows.

Xiaowei Yang received his Ph.D. degree from Shanghai Jiao Tong University in 2011 with Prof. Zi-Feng Ma. He carried out research on tunable layered graphene gel in Prof. Dan Li's group at Monash University (2009–2014) and is currently a professor at Tongji University. His current research interests are centered on the synthesis and properties of 2D soft materials and their applications in energy storage and conversion, nanofluidics, and biomedicines.

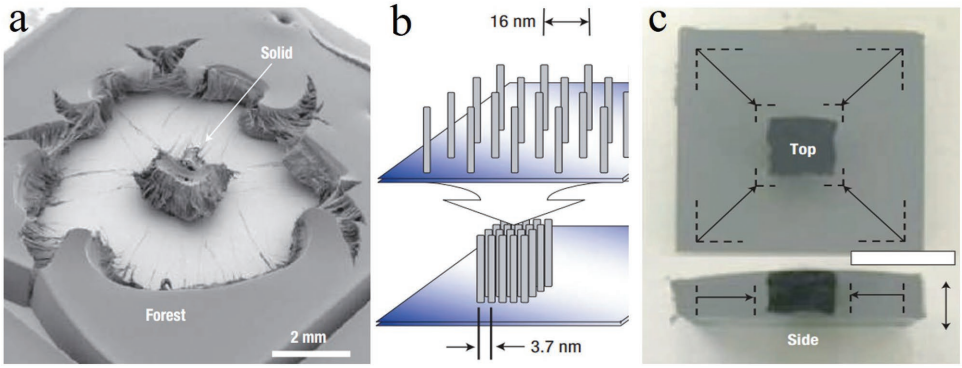

Figure 1. Liquid-induced collapse of densely packed and aligned single-walled carbon nanotubes (SWNTs).[42] a) Scanning electron microscopy (SEM) image of SWNT forest collapse from liquid, b) schematic of the collapse, and c) pictures of the lateral dimension decrease. Reproduced with permission.[42] Copyright 2006, Nature Publishing Group.

Compared with traditional carbon materials, graphene, with a 2D configuration together with its high electrical conductivity and ultralarge theoretical SSA, was widely considered as an ideal electrode material for ECs.[44] More importantly, the unique 2D structure is a great advantage for assembling a dense electrode, leading to its great potential in compact capacitive energy storage.[45] For instance, a high packing density of 1.58 g cm^{-3} for a porous graphene macroform (HPGM) electrode can be produced by evaporation-induced drying of a graphene hydrogel.[46] The HPGM electrode-based ECs revealed an excellent volumetric capacitance of 376 F cm^{-3} at 0.1 A g^{-1} in an aqueous system (6 M KOH) (**Figure 2**).

Recently, beyond graphene, novel 2D metal-inclusive materials (such as MXenes and transition-metal dichalcogenides) as negative electrode materials have demonstrated favorable cation-intercalation capacitance in compact energy storage systems. For example, MXene Ti_3C_2 and 1T MoS_2 films with densities of 3.6–3.8 and 5 g cm^{-3} have revealed appealing cation-intercalation capacitances of 900 and 700 F cm^{-3} in sulfuric acid electrolyte, respectively.[25,27] Obviously, a high packing density indicates a superior volumetric capacitance (**Figure 3**a).

3. The Essential Effect of Pore on the Density and Capacitance

3.1. The Tradeoff between the Density and Pores

The density and pores of the electrode have a competitive relationship. Electrodes with a low packing density usually possess an abundance of voids owing to excessive mesopores and macropores. In contrast, an ultrahigh density usually leads to a small pore size or narrow channels. For example, graphite is an assembly of 2D graphene with dense face-to-face parallel stacking, with a high density of ≈2.2 g cm^{-3} and a very narrow average interplanar spacing of ≈0.335 nm. The density decreased as the average interplanar spacing increased (Figure 3b).[19] Generally, the densities of the commercial AC-based electrodes are ≈0.5 g cm^{-3}, which is equivalent to graphene films with an average pore size of 1.47 nm. Therefore, for graphene-based dense electrodes, the average pore size for the range of micropores should not be larger than 1.5 nm to obtain more compact electrodes than their commercial counterpart.

3.2. The Relevance between the Pore Features and the Capacitance

The pores are not only related to the density of the electrodes, but their features, such as pore size, connectivity, and wettability, are also related to the accessibility of the electrolyte ions, which ultimately affects the capacitance.

Pore Size: Initially, high SSA together with an increase in the pore volume is a priority in achieving a high capacitive performance. The SSA largely arises from a complex network of internal pores with different sizes, such as macropores (>50 nm in size), mesopores (2–50 nm), and micropores (<2 nm).[47] Macroporous cores as ion-buffering reservoirs provide avenues for electrolyte transport into the interior of active materials. The moderate size of the mesopores could facilitate the adsorbate accessibility by providing effective transport channels for the diffusion of electrolyte ions into the mesopores. In contrast, micropores play a more important role in the charge accommodation of the adsorption-based processes through controlled diffusion and molecular sieve effects.[48,49] For the various role of different pores, Cheng and co-workers reported a 3D aperiodic hierarchical porous carbon material showing a unique structure with a total pore volume of 0.69 cm^3 g^{-1}, a micropore volume of 0.3 cm^3 g^{-1}, and a micropore-to-total-pore-volume ratio of 0.43. This novel material displayed high-rate electrochemical performances, indicating a good strategy to balance the pores with different sizes.[49] Several prominent studies have also reported an important capacitive contribution from micropores. For conventional porous carbon materials, the optimal pore size of 0.8–2.0 nm is available for the electroadsorption of hydrated ions.[50] With regard to the organic electrolytes, a high capacitance is realized based on CDC materials with a pore size of ≈0.7 nm.[51] Notably, the sub-nanometer-sized pores of 0.55–0.70 nm by liquid-mediated engineering enable the electrolyte ions to intercalate into the smaller pores, resulting in an ultrahigh capacitance in both aqueous and organic electrolytes.[19]

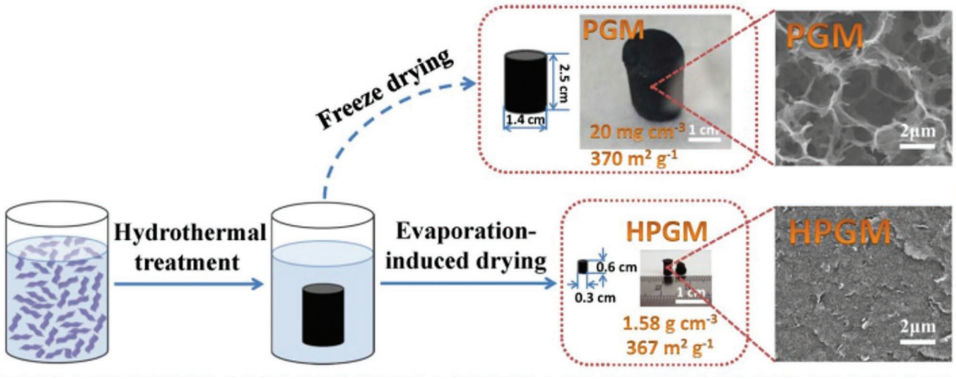

Figure 2. Schematic of the formation of self-assembled highly dense but porous graphene-based monolithic carbon (HPGM) with different drying processes, and SEM images of different resultants. Reproduced with permission.[46] Copyright 2013, Nature Publishing Group.

Pore Connectivity: In addition to the size, the influence of other pore features, such as the connectivity, wettability, uniformity, and distribution on the capacitance, cannot be ignored. A connected porous architecture means that open and continuous porous structures, which can facilitate the rapid ionic transport within the pores to provide access for the ions to reach the active materials surface, are present, and it is advantageous for achieving high specific capacitance for dense electrodes and ultrahigh power density.[52] A previous study reported that the importance of the connectivity of the pores exceeds the importance of the pore size to in ensuring the fast interfacial faradaic reaction in compact electrodes.[53–55]

Wettability: The wettability toward the liquid electrolyte may be diminished in the presence of micropores because conflicting forces at the sub-nanoscale. A higher level of wettability for micropores will not only decrease the system resistance to improve the power performance but would also increase the contact surface of the electrolyte and active materials, which would enhance the energy storage capabilities.[19]

3.3. The Mechanisms of Ion Transport in Micropores

In charge/discharge process, the main function of the micropores is to accommodate charge storage and strengthen the capacitance.[49] When the size of pores decreases toward the size of solvated ions, the physical characteristics of mass storage/transport processes for the ions can change drastically generating anomalous properties in the nanopores.[56] Consequently, basic understanding of ion transport in the micropores is essential to improve the capacitive energy storage. The anomalous increase in carbon capacitance in organic electrolyte for most pore sizes below 1 nm has been reported, which is mainly due to ion dissolution.[56] Presser and Paris and coworkers demonstrated a combined experiment and simulation method and simulated scattering approach to provide evidence of the partial dissolution of hydrated Cs^+ and Cl^- ions in mixed micromesoporous carbons with an average pore size above 1 nm.[57] Meanwhile, for electrolytes with a significant difference between the anions and cations, a smaller corresponding surface area is accessible to the larger ions during electrosorption.[58] Furthermore, the electrochemical quartz crystal microbalance technique was also introduced to offer more information on the ion dynamics in nanoporous carbon materials during the charge/discharge processes. For the neat 1-ethyl-3-methylimidazolium bis(trifluoromethanesulfonyl)imide (EMI-TFSI) electrolyte, charge is efficiently stored because the polarization is sufficiently large. Regarding the solvated EMI-TFSI, the results signify that the EMI^+ cation possesses a higher mobility than the $TFSI^-$ anion.[59] Recently, new ionic liquids (ILs) with redox

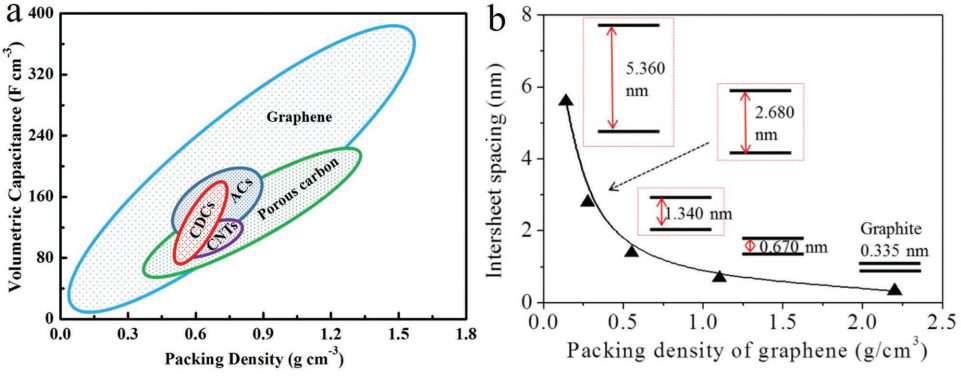

Figure 3. a) Volumetric capacitance and packing density of electrodes based on different carbon materials for symmetric ECs. b) Theoretically describing the relation between intersheet spacing and packing density of graphene in a face-to-face arrangement. Reproduced with permission.[19] Copyright 2013, AAAS.

moieties on both ions used as electrolytes in ECs have demonstrated potential for high-capacity/high-rate charge storage with a wide electrochemical window. The cation and anion of the biredox ILs could bear moieties that undergo fast reversible redox reactions, achieving a bulk-like redox density.[60] The aforementioned basic understanding of the ion transport in the micropores offers a great opportunity for designing optimized porous materials for high-performance ECs.

Consequently, one of the main scientific and technical challenges toward realizing excellent volumetric performance is manufacturing porous and interconnective structures that can couple with the solvated ions in high-density electrodes. During the past few years, a variety of pore-engineering strategies have been employed to fabricate a dense electrode while maintaining a porous architecture, providing effective pathways for electrolyte ion diffusion and resulting in suitable volumetric performance.

4. Pore Engineering

4.1. Engineering of Pore Sizes

4.1.1. Mechanical Compressing

As an effective method to increase the density of an electrode, mechanical compression can reduce the volume of macropores and mesopores inside a loosely packed electrode. Beguin's group prepared a low-porosity AC material and compacted aggregates of multiwalled nanocapsules, resulting in a low SSA (273 m^2 g^{-1}). The dense electrode (0.9 g cm^{-3}) fabricated by pressing this porous AC material (90 wt%) together with a binder (10 wt%) allowed a high volumetric capacitance of 180 F cm^{-3} and an $E_{vol\text{-}electrode}$ of 6.66 Wh L^{-1} in a 1.0 M H_2SO_4 electrolyte.[29] Facing the disadvantage of low density (0.3 g cm^{-3}) for SWNTs, Zhou et al. employed a mechanical densification method to attain an aligned-SWNT electrode. As a result, the SWNT electrode (0.5 g cm^{-3}) yielded a high volumetric capacitance of 130 F cm^{-3} with $E_{vol\text{-}electrode}$ of 75 Wh L^{-1} in a 3 M $EMIBF_4$/PC electrolyte.[17] Ruoff and co-workers reported that the density of activated microwave-expanded graphite oxide (aMEGO) sample can also be increased from 0.34 to 0.75 g cm^{-3} by mechanical compression. The dense aMEGO electrode delivered a high volumetric capacitance of 110 F cm^{-3} and $E_{vol\text{-}electrode}$ of 48 Wh L^{-1} in an organic electrolyte.[61]

4.1.2. Capillary Densification

Compression by capillary pressure through the regulated evaporation of different solvents is another unique method toward decreasing an excess of mesopores and macropores, together with increasing the packing density of the electrode. Hata and co-workers densified a vertically aligned SWNT forest synthesized by a water-assisted chemical vapor deposition method to fabricate a high-density solid form (0.5 g cm^{-3}). This type of SWNT electrode (thickness of 100 µm) presented a volumetric capacitance of 80 F cm^{-3} with an energy density of 47 Wh L^{-1} at a high voltage of 4 V.[62]

For porous carbon materials, Hu and co-workers developed an in situ templating method to obtain hierarchical CNC with coexisting porous structures ranging from micropores to macropores;[63,64] then, by collapsing the macropores via capillarity (collapsed carbon nanocage (CCNC)), they increased the density up to 1.32 g cm^{-3}. A high volumetric capacitance of 233 F cm^{-3} with a maximal $E_{vol\text{-}electrode}$ of 130 Wh L^{-1} was obtained at 1 A g^{-1} in the neat $EMIMBF_4$ electrolyte, with an electrode thickness of 38 µm (3.5 mg cm^{-2}). Even by increasing the thickness from 38 to 115 µm (10.6 mg cm^{-2}), the volumetric capacitance retained 206 F cm^{-3} at 1 A g^{-1} with the maximal $E_{vol\text{-}electrode}$ of 114 Wh L^{-1}. The maximal $E_{vol\text{-}stack}$ was significantly enhanced from 48 to 73 Wh L^{-1} because of the increase in f and was comparable to that of lead-acid batteries (50–90 Wh L^{-1}) (**Figure 4**).[35]

4.1.3. Filling Surplus Pores with Active Components

The incorporation of additional capacitive components in the mesopores and macropores also realized high volumetric performance as a consequence of optimizing the pore structures. The existence of new components with capacitive characteristics is feasible to further increase the capacitance, fully utilizing the advantages of the different components. Polyaniline (PANI) is one of the most widely studied pseudocapacitive materials for its high theoretical capacitance and fast redox protonation/deprotonation reactions.[65–67] To combine the PANI filling and the capillary force compressing, a compact PANI/graphene composite with packing density as high as 1.5 g cm^{-3} was obtained by controlling ANI monomer polymerization in graphene monoliths and eliminating the mesopores of 3.5 nm (**Figure 5**). This dense PANI/graphene composite electrode yielded a high volumetric capacitance of 802 F cm^{-3} in a symmetric two-electrode system with aqueous electrolyte.[68]

4.1.4. Optimizing the Micropore

The aforementioned strategies for controlling pore size were to decrease the size of macropores and mesopores in low-density electrode. For a compact electrode, an appropriate porosity is needed in the high-density monolith electrode to decrease the electrolyte-ion transport distance. Manufacturing a microporous network by the template method in a compact monolith electrode is another effective way to achieve a superior volumetric performance. Yang's group introduced $ZnCl_2$ as an ideal pore-forming agent to develop tunable porous graphene monolith (PaGM) materials with a density of 0.87 g cm^{-3} (**Figure 6**). To get an excellent volumetric energy density, a series of thick pellet electrodes with different thickness from 100 to 800 µm were directly sliced from the PaGMs to evaluate its potential in the field of compact capacitive energy storage. With the precise adjustment in the porosity and density, as well as thickness, which consequently results in optimum ion transport, a $E_{vol\text{-}stack}$ of 64.7 Wh L^{-1} was achieved from 400 µm thick PaGM pellet electrode in neat ionic liquid electrolyte at an operating voltage of 4.0 V.[69] This is also typical for the design of an electrode with sufficient consideration for pore engineering.

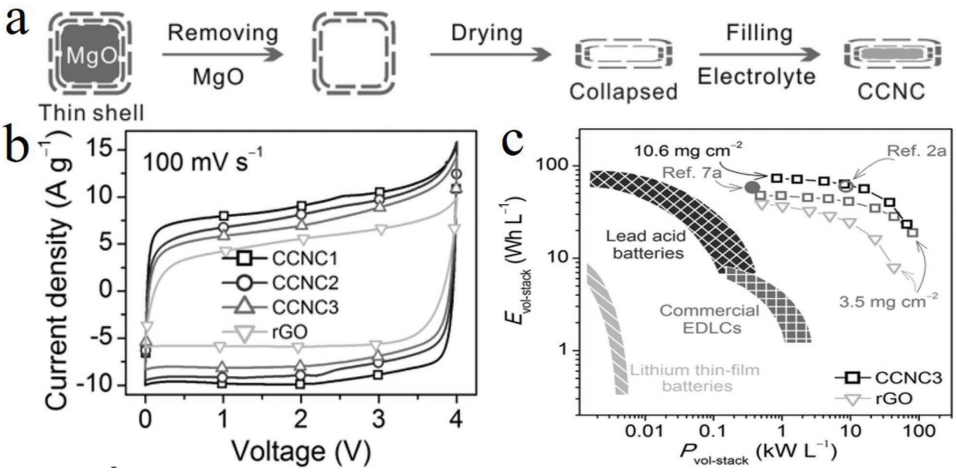

Figure 4. Collapsed carbon nanocages (CCNCs) via capillarity.[35] a) Schematic of the preparation of CCNC, b) cyclic voltammogram curves, and c) volumetric performance in Ragone plots. Reproduced with permission.[35] Copyright 2017, Wiley-VCH.

Sintered TiC ceramic plates as a precursor of CDC possess an ultrahigh density of 4.93 g cm^{-3}. Like the above examples, CDC has shown excellent performance as an electrode material since its pore size (0.5–3 nm) can be fine-tuned by controlling the preparation conditions.[36–38] The CDC electrode with an average pore size of 0.68 nm showed high volumetric capacitance of 160 and 180 F cm^{-3} at a thickness of 2 µm for aqueous (1 M H_2SO_4) and organic (1 M $TEABF_4$) electrolytes, respectively.[36] Beyond that, 2D MXenes etched by hydrofluoric acid (HF) also exhibit sub-nanometer channels between layers.[70] The dense MXene (Ti_3C_2) film as a negative electrode demonstrates a favorable cation-intercalation capacitance of 442 F cm^{-3} at 2 mV s^{-1} in a three-electrode cell due to the high electrical conductivity and packing density (3.4 g cm^{-3}).[24]

4.1.5. Incorporation of Spacers to Enlarge Micropores

Solid capacitive materials were also introduced to prepared composite materials based on MXenes by using different strategies with the aim of creating aligned channels and achieving a high volumetric performance. A flexible and conductive dense MXene/graphene (reduced graphene oxide, rGO) film was presented by using electrostatic self-assembly between negatively charged titanium carbide Ti_3C_2 and positively charged rGO nanosheets modified with PDDA. Therefore, the self-restacking of the Ti_3C_2 nanosheets was effectively prevented, leading to the accelerated diffusion of electrolyte ions. The free-standing MXene/graphene electrode with a packing density of 4.1 g cm^{-3} displayed a volumetric capacitance of 1040 F cm^{-3} at a scan rate of 2 mV s^{-1} and could maintain 634 F cm^{-3} at 1 V s^{-1} in a three-electrode system with 1 M H_2SO_4 electrolyte.[71] Gogotsi's group also presented a facile method for the synthesis of Ti_3C_2/polypyrrole (PPy) composites with aligned PPy chains between Ti_3C_2 layers. A 13 µm thick PPy/Ti_3C_2 composite electrode yielded a high volumetric capacitance of 1000 F cm^{-3} in H_2SO_4 electrolyte within a three-electrode setup.[72]

4.2. Engineering of Pore Connectivity

4.2.1. Forming 3D Pores with Crossed Nanoholes

With face-to-face parallel stacking, the ion transport across the 2D nanosheet plane might occur in the vertical direction. Holey nanosheets, which are defined as an abundance of nanoholes distributed in the nanosheets, display great promise for forming connective and porous structures that facilitate electrolyte ion diffusion across the 2D plane and provide effective access to the inner electrode.[73] Hu and co-workers used a chemical-free and catalyst-free procedure to synthesize holey graphene nanosheets. The nanohole size (0.9–1.7 nm) and distribution in the graphene sheets could be tuned by controlling the preparation process (**Figure 7**). The 2D nanoholes (>1.3 nm) can be viable pathways for the access of electrolyte ions (EMI:TFSI). Due to the presence of the nanoholes, the obtained holey graphene electrode with a high packing density of 1.2 g cm^{-3} demonstrated a maximal volumetric energy density of 12 Wh L^{-1} at 3 A g^{-1}, which is six times that of a common graphene film (≈2 Wh L^{-1}).[54] Additionally, the volumetric performance of this holey graphene film can be further increased by optimizing the preparation conditions.

As shown in **Figure 8**, SWNTs were employed as a bridge in building SWNT-bridged graphene 3D building blocks to increase the accessible surface area and allow for fast electrolyte ion diffusion. KOH activation plays a key role in creating nanoscale pores in the graphene nanosheets, which significantly increase the ion accessibility. The resulting free-standing graphene/SWNT films have a high electrical conductivity of 394 S cm^{-1} and an ideal mass density of 1.06 g cm^{-3}. With the reasonable density and optimized 3D porous structure, the graphene/SWNT film as an electrode of ECs displayed a high volumetric capacitance of 211 F cm^{-3} at a current density of 0.5 A g^{-1} and a relatively large value of 105 F cm^{-3} at 20 A g^{-1}. This 3D electrode showed a high $E_{vol\text{-}electrode}$ of 117.2 Wh L^{-1} at power density of 424 kW L^{-1} in 4.0 V ion liquid electrolytes.[55]

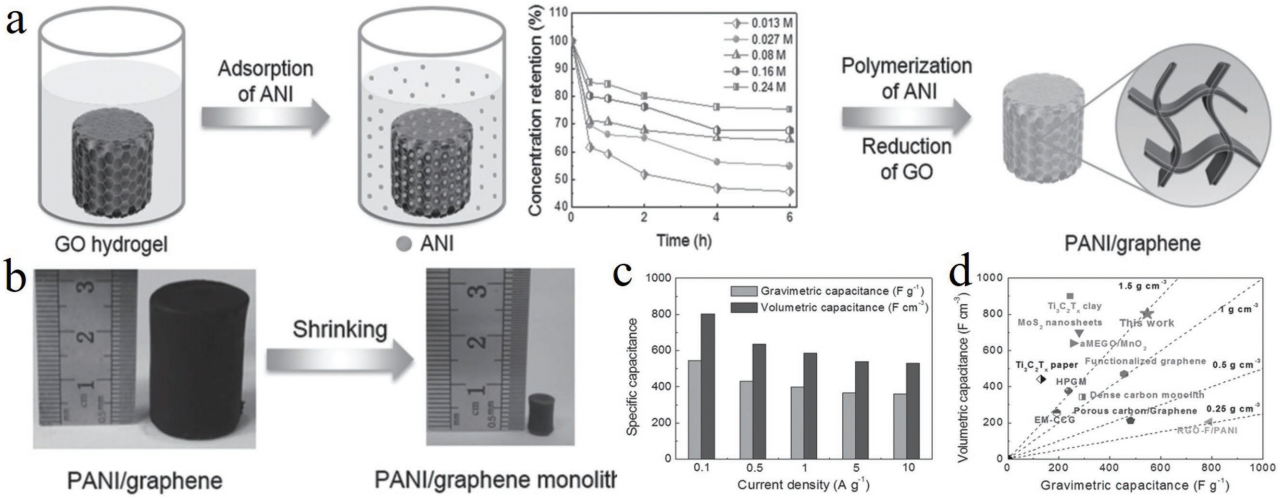

Figure 5. PANI/graphene composite monoliths.[68] a) Schematic of the synthesis process, b) condensing the PANI/graphene via vacuum drying, and c,d) volumetric capacitance at different current densities and the comparison with previous work. Reproduced with permission.[68] Copyright 2015, Wiley-VCH.

4.2.2. Tailoring Aligned Pores

Graphene shows a great advantage for manufacturing dense electrode due to its 2D configuration,[45] whereas the easy restacking of graphene always resulted in a dense but nonporous structure and especially a poor connectivity. With regard to the traditional horizontal orientation of graphene on the current collector, due to the long path length and close interlayer gap distance, the electrolyte ions cannot easily diffuse horizontally. Vertically oriented graphene on the current collector with a suitable porous and connectivity structure is believed to shorten the paths of the electrolyte ions in the graphene layers and facilitate the rapid ion mobility.[74] Lee's group fabricated a vertically aligned reduced graphene oxide (VArGO) electrode with a high packing density (1.18 g cm^3) through a simple rolling and cutting process. As shown in **Figure 9**, the SWNTs were also introduced to avoid the tight layer-by-layer restacking of rGO. The dense VArGO electrode showed a high volumetric capacitance of 171 F cm^{-3} as well as a volumetric energy density of 7.43 Wh L^{-1} in an aqueous electrolyte. In particular, the ideal volumetric performance was maintained even as the film thickness increased due to the vertically aligned and opened-edge connectivity of the structure, which provided a very fast electrolyte ion diffusion.[53]

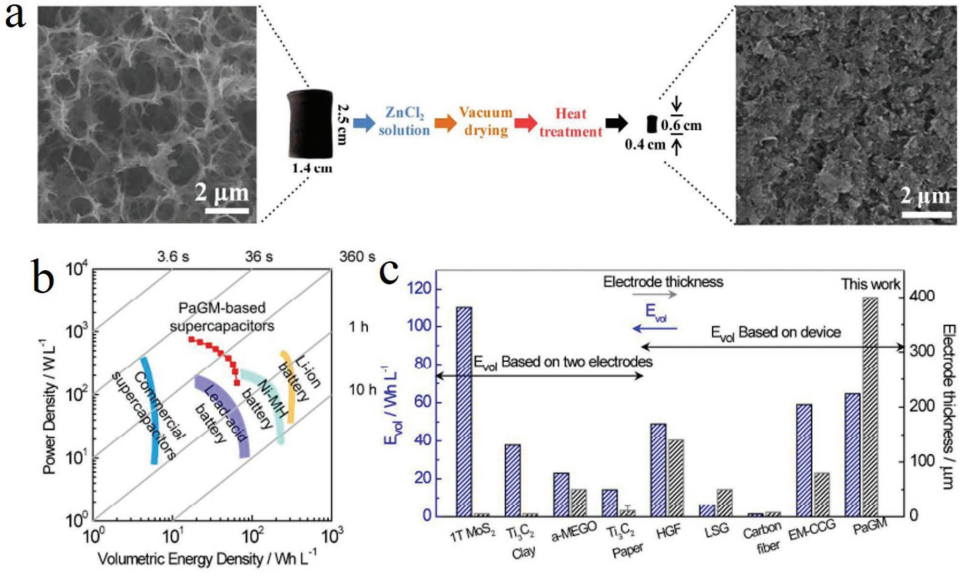

Figure 6. Density and porosity-controlled graphene monoliths.[69] a) Schematic of the preparation of graphene monolith via $ZnCl_2$ used as a pore-forming agent, b) volumetric performance in Ragone plots, and c) volumetric performance compared with previous works. Reproduced with permission.[69] Copyright 2016, Royal Society of Chemistry.

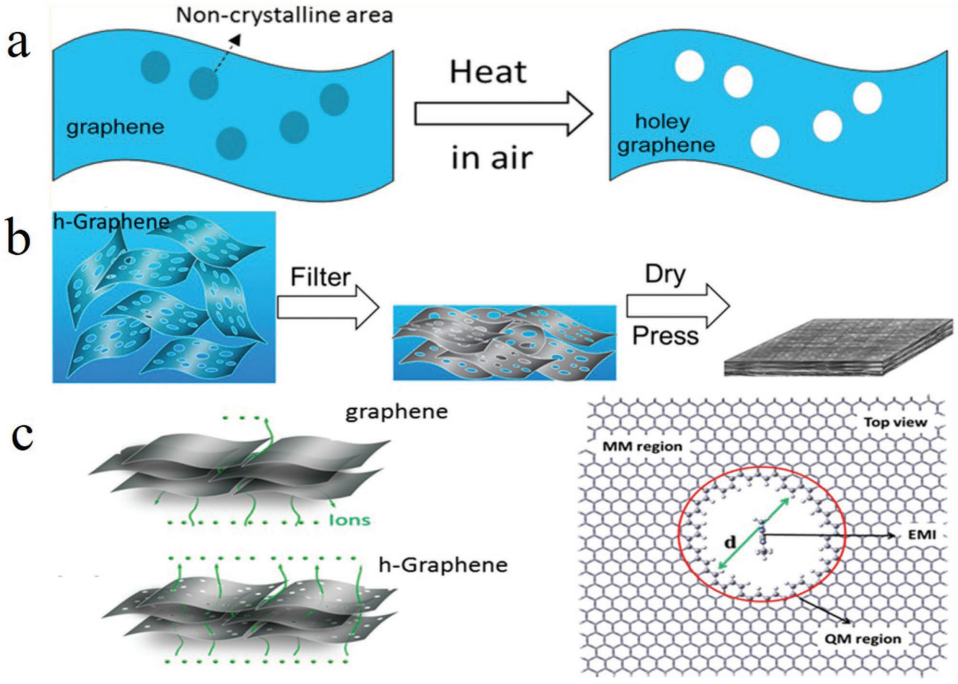

Figure 7. a) Schematic of the synthesis of holey graphene and b) electrode fabrication, and c) schematic representation of the ion migration mechanism. Reproduced with permission.[54] Copyright 2014, American Chemical Society.

4.3. Liquid Mediated Engineering of Sub-nanopores

Conventional processing of the supercapacitor involves the following discrete steps: the formation of porous carbon by top-down methods, the formation of the electrode, and the infiltration of electrolyte; therefore, the narrow pores will only be accessed through an appreciable "solution resistance" arising from hindered or restricted electrolyte diffusion.[48] This inevitable issue of "wettability" in ultrasmall pores and the porosity collapse from the relaxation of surface stresses as well as the perturbation of the interconnected structure that facilitates electron conduction will result in an even greater negative effect on the capacitance and rate capability when the electrodes increase in thickness.[36]

To better harmonize the electrolyte and sub-nanopores, the engineering of nanopores by controlling the exceptional colloidal forces of the chemically converted graphene (CCG) was developed by Li's group.[19] Chemically, graphene is essentially a 2D conducting polymer with a large, molecular configuration. Because of the combination of the 2D configuration and the ultralarge molecular size and self-contained functional groups, CCG sheets were able to self-gel at the solid–liquid interface during filtration, leading to a new class of oriented, conductive hydrogel films with unprecedented mechanical, electrical, and anisotropic stimuli-responsive properties. Ascribed to the hydration effect of CCG, the face-to-face stacked CCG hydrogel film can remain largely separated by the presence of intercalated water molecules, which generate repulsive forces

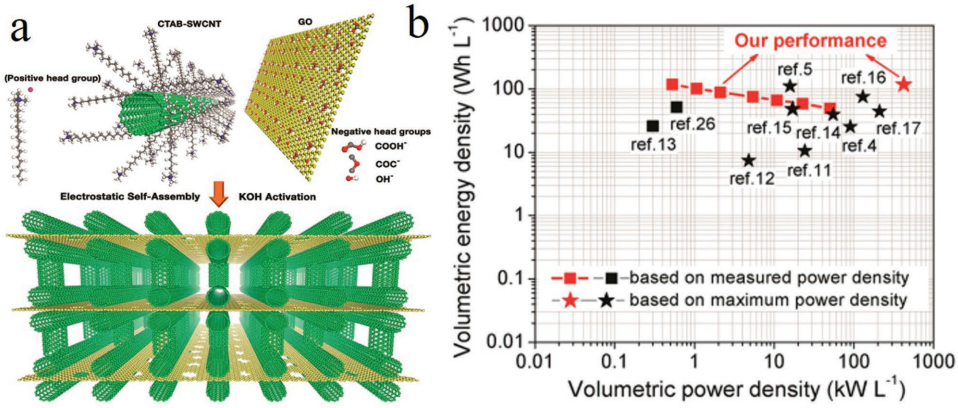

Figure 8. Carbon-nanotube-bridged graphene. a) Schematic of fabricating the hybrid nanostructure and b) volumetric performance compared to previous works. Reproduced with permission.[55] Copyright 2015, American Chemical Society.

sufficient to mitigate the restacking of graphene nanosheets. The resultant graphene hydrogel film can provide an open porous structure, allowing the electrolyte ion to easily access the surface of individual nanosheets.[75]

Taking advantage of the unique colloidal assembly behavior of CCG, we further demonstrated that dense but porous films can be readily formed by capillary compression of the adaptive graphene hydrogel films in the presence of nonvolatile and volatile liquids.[19] Upon evaporation, the polymeric steric force and hydration force will play a crucial role in the "soft" strategy, leading to the simultaneous control of the packing density and interplanar spacing in response to the residual nonvolatile liquid. Due to the fluid nature of liquids, the continuous liquid network remained within the film during the drying process, facilitating the connective ion transport channels and increasing the interface with the electrolyte. The packing density of these electrolyte-mediated CCG (EM-CCG) films can be finely controlled from 0.069 to 1.33 g cm^3 by changing the ratio of the volatile and nonvolatile liquids, while the density of the fully dried CCG films is 1.49 g cm^3 (**Figure 10**). More significantly, the extent of the fluctuation in capacitance strongly proved that the preincorporated liquid plays an indispensable role. In a two-electrode cell with 1 M H_2SO_4 electrolyte, the dense CCG gel film (1.33 g cm^{-3}) delivered a high C_{vol} of 255.5 F cm^{-3} at a current density of 0.1 A g^{-1}. More pronounced at a large operation rate of 100 A g^{-1}, the dense CCG gel film still displayed a good C_{vol} of 133 F cm^{-3}. The dense graphene gel film exhibited a volumetric capacitance of 261.3 F cm^{-3} and $E_{vol\text{-}electrode}$ of 110.3 Wh L^{-1} in 3.5 V organic electrolytes. As the thickness increased to 80 µm (density 1.25 g cm^{-3}, mass loading 10 mg cm^{-2}) a tremendous volumetric performance was demonstrated with a high $E_{vol\text{-}stack}$ of 59.5 Wh L^{-1} corresponding the $P_{vol\text{-}stack}$ of 8.6 kW L^{-1}.

Duan and co-workers reported that a 3D holey graphene framework (HGF) was fabricated by nanopore etching in graphene and the self-assembly of graphene combined with a liquid-mediated approach (**Figure 11**). With the advantages of an excellent mechanical stability and highly porous structure, the resulting HGF can be greatly compressed to form a compact HGF film with a packing density of 0.71 g cm^{-3}. The size, connectivity, and wettability of the pores in the dense electrode were simultaneously well adjusted. Because of the excellent ion diffusion and high electrical conductivity, the thicker HGF electrode (thickness 140 um) in an assembled device can deliver an $E_{vol\text{-}stack}$ of 49.2 Wh L^{-1} in $EMIMBF_4$/AN electrolyte for the fully assembled device.[76] In addition, we also prepared compact PANI-CCG films with high connectivity and a porous structure by controlled capillary compression based on a liquid-mediated method. The dense PANI-CCG gel film (1.28 g cm^{-3}) also provided a combination of high volumetric capacitance (572 F cm^{-3} at current density of 5 A g^{-1}) and high rate capability (548 F cm^{-3} at 100 A g^{-1}) in 1 M H_2SO_4 electrolyte attribute to its high pore connectivity.[52] This type of architecture facilitates the fabrication of compact and thicker electrode without significantly sacrificing the capacitance.

Gogotsi and co-workers demonstrated a novel approach of producing hydrophilic MXene (Ti_3C_2) materials using a solution of LiF and HCl to etch aluminum from the MAX phase of Ti_3AlC_2. Owing to the role of surface terminations, such as OH, O, and F, in MXenes, the Ti_3C_2 films display a hydrophilic

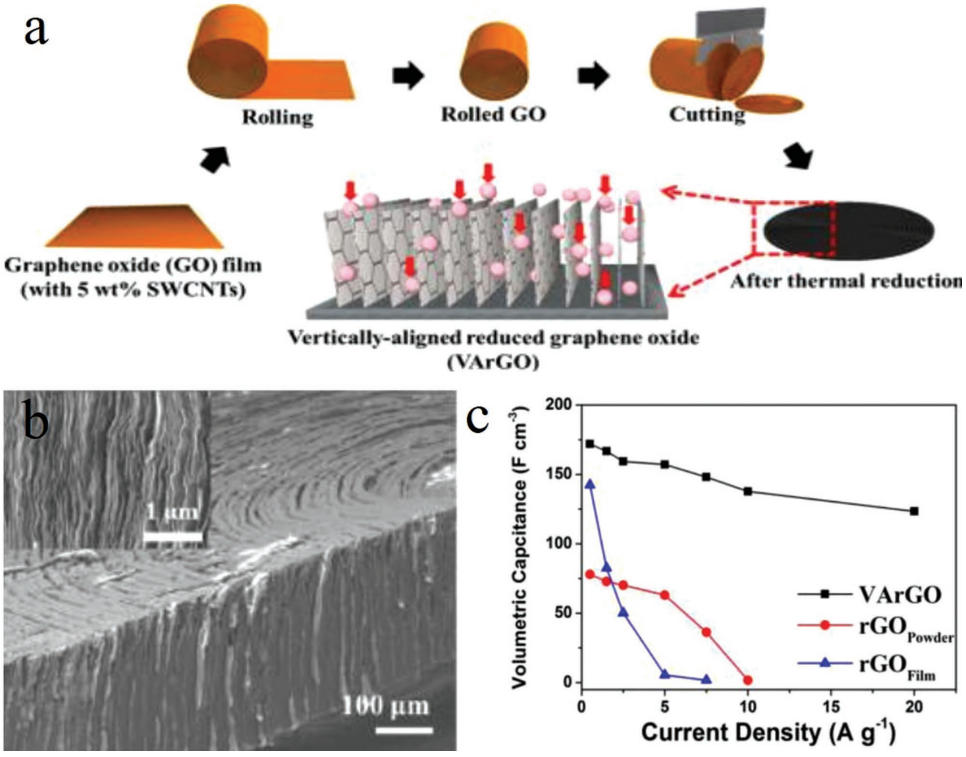

Figure 9. Vertically aligned reduced graphene oxide electrode (VArGO). a) Schematic of the preparation of VArGO, b) cross-sectional images of VArGO, and c) volumetric capacitance of VArGO. Reproduced with permission.[53] Copyright 2014, American Chemical Society.

nature. Within a potential range of –0.35–0.2 V (1 M H_2SO_4 electrolyte), high-density 2D Ti_3C_2 films (3.7 g cm^{-3}) with thicknesses of 5 µm presented an exciting cation intercalation capacitance of 900 F cm^{-3} in a three-electrode configuration, demonstrating their great potential as electrode materials for energy storage with an ideal volumetric performance.[25] To further enhance the volumetric capacitance of MXene materials,[19] they also prepared Ti_3C_2 hydrogel electrodes by adopting the liquid-mediated approach, and this approach transported electrolyte ions to electrochemically active sites between compact MXene sheets. An ultrahigh volumetric capacitance of 1500 F cm^{-3} was obtained at 2 mV s^{-1} for a 3 µm $Ti_3C_2T_x$ hydrogel film (density 4 g cm^{-3}, mass loading 1.2 mg cm^{-2}) in a potential window of 1 V (–1.1 to –0.1 V vs Hg/Hg_2SO_4) in 3 M H_2SO_4 electrolyte. The $Ti_3C_2T_x$ hydrogel film electrode (13 µm, 5.3 mg cm^{-2}) also delivered a high C_{vol} at 2 mV s^{-1} (**Figure 12**).[26]

Indeed, as previously mentioned, there have been many advances in pore engineering toward obtaining high-performance capacitive energy storage with different dense electrodes (>0.5 g cm^{-3}) (**Table 1**). The guidelines for designing and developing compact electrodes with high volumetric performance involve optimizing the pore features such as the size, connectivity, and wettability, to accommodate the electrolyte ions. However, there are still challenges that still need to be further explored.

5. Challenges and Prospect

5.1. Challenges

The density and pore characteristics of an electrode are important parameters concerning the volumetric performance of the whole electrode. How to efficiently balance the tradeoffs between density and porosity of different materials remains a great challenge, though several detailed methods of pore engineering have been previously proposed. The mechanism of ion transport and adsorption of ultradense and sub-nanoporous electrodes should be determined. The pore distribution of thick electrodes (>10 mg cm^{-2}) should be more hierarchical than thin ones, to satisfy the different ion transport resistance with diverse thicknesses. For metal-inclusive 2D materials, such as dense MXenes, it is important to determine the best methods to engineer the nanoporous structure to achieve an ultrahigh capacitance for organic electrolyte ions or anions.

Notably, the density and pore characteristics of the electrode are easily affected by the fabrication procedure from active materials to an integrated electrode because these powdered active materials require preparation with a binder and conductive additive. The best method for engineering the relationships between the materials and binders together with other additives to obtain the suitable porosity with a high density must be determined. It is also important to determine whether compressing the electrodes causes the collapse of pores and reduces the conductive paths.

5.2. Prospects

When the relationship between the electrode thickness and volumetric energy density of $E_{vol\text{-}electrode}$ and $E_{vol\text{-}stack}$ was considered, the volume fraction of the active electrode needed to be considered (see Equations (2) and (3)) because the $f_{electrode}$ increased with the electrode thickness and the other components of ECs remained unchanged. However, both the $C_{wt\text{-}C}$ and C_{vol} generally decreased with increasing thickness of the electrode. This phenomenon was particularly prominent in high-density materials. Previous research has demonstrated that the pores with different sizes played a unique role concerning the capacitance performance; in particular, the amazing increasing of capacitance of charge storage in sub-nanometer pores can be attributed to the desolvation effect.[48,49,56] Constructing an

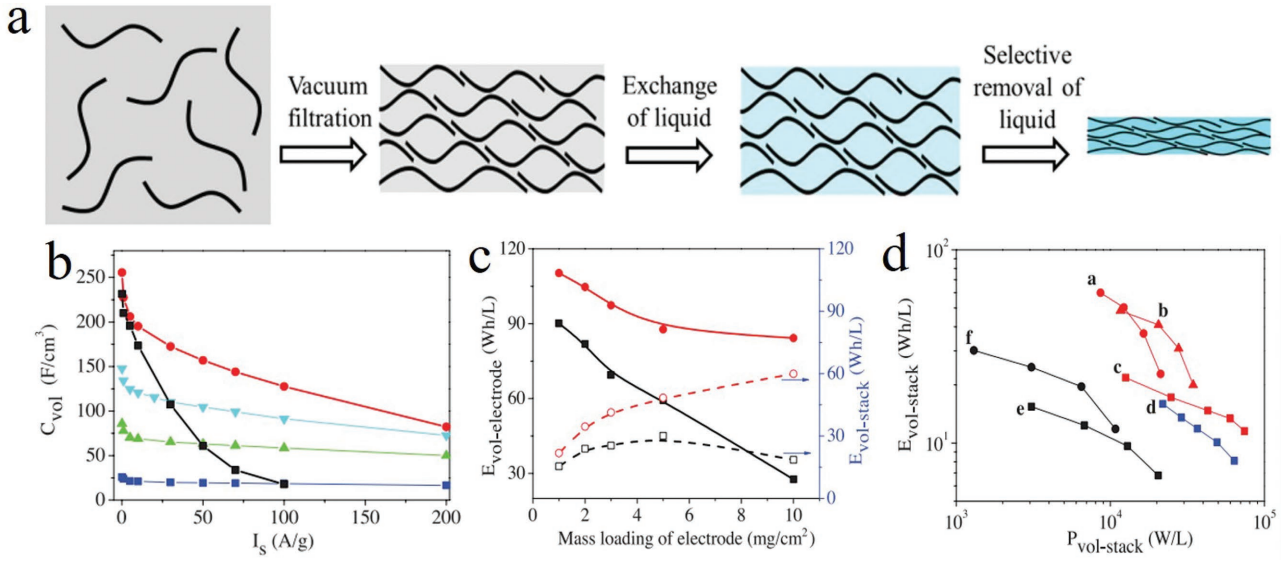

Figure 10. Electrolyte-mediated graphene gel film. a) Schematic of fabricating the graphene film, and b–d) electrochemical characterization. Reproduced with permission.[19] Copyright 2013, AAAS.

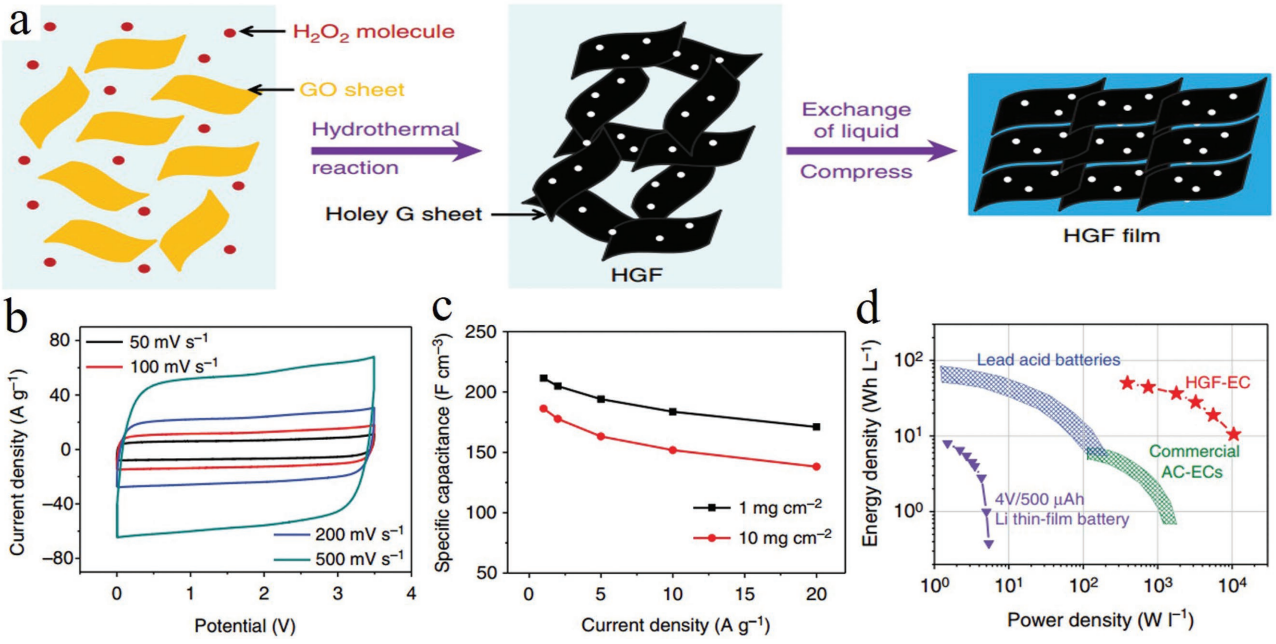

Figure 11. Holey graphene framework (HGF). a) Schematic of the preparation process of HGF film, b) cyclic voltammogram curves in organic electrolyte, c) volumetric capacitance of HGF with different mass loading, and d) volumetric performance in Ragone plots. Reproduced with permission.[76] Copyright 2014, Nature Publishing Group.

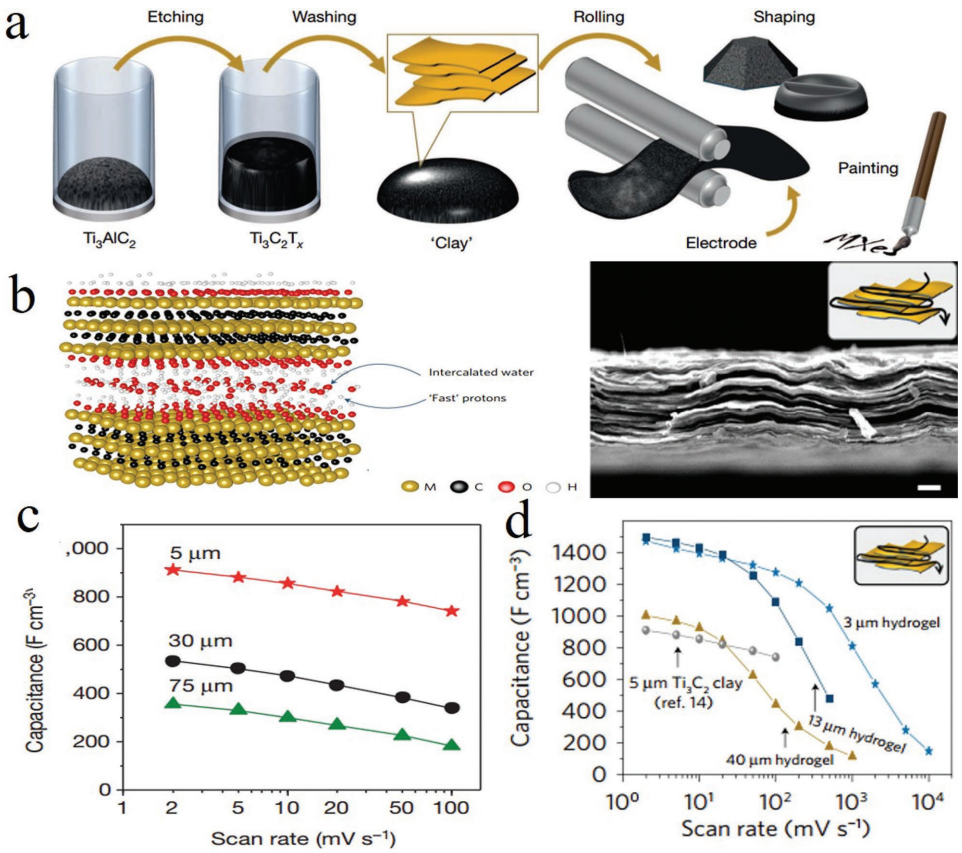

Figure 12. a) Schematic of MXene "clay" synthesis, b) schematic illustration of MXene hydrogel structure and SEM image, c) volumetric performance of rolled, free-standing MXene film, and d) volumetric capacitance of MXene hydrogel films with different thickness.[26] a,c) Reproduced with permission.[25] Copyright 2014, Nature Publishing Group. b,d) Reproduced with permission.[26] Copyright 2017, Nature Publishing Group.

Table 1. Volumetric performance of reported dense electrodes for symmetric ECs.

Materials	Density [g cm^{-3}]	Electrolyte/ operation voltage [V]	Scan rate	$C_{wt\text{-}c}$ [F g^{-1}]	C_{vol} [F cm^{-3}]	$E_{vol\text{-}electrode}$ [Wh L^{-1}]	f	$E_{vol\text{-}stack}$ [Wh L^{-1}]	Reference
AC	0.5	EMIMBF$_4$ [3.5 V]	1 A g^{-1}	207	104	44	–	–	[15]
ALG-C	0.9	1 M H_2SO_4 [1.0 V]	2 mV s^{-1}	400	200	6.66	–	–	[30]
MHCN	0.78	1 M EMIMBF$_4$/AN [2.5 V]	0.5 A g^{-1}	103	80	17.3	–	–	[77]
CDC	0.64	1 M H_2SO_4 [1.0 V]	–	–	160	-	–	–	[37]
	0.64	1 M TEABF$_4$/PC [2.5 V]	–	–	180	–	–	–	[37]
CDC	0.53	EMIMTFSI [3.0 V]	0.3 A g^{-1}	160	85	26.5	–	–	[51]
SWNTs	0.5	3 M EMIBF4/PC [3.0 V]	0.1 A g^{-1}	260	130	75	–	–	[17]
SWNT arrays	0.5	Et$_4$NBF$_4$/PC [4.0 V]	1 A g^{-1}	160	80	47	0.53	24.7	[62]
Porous carbon	0.93	1.5 M Et$_4$NBF$_4$/AN [2.5 V]	2 mV s^{-1}	156	145	29	–		[32]
CCNC	1.32	EMIMBF$_4$ [4.0 V]	1 A g^{-1}	156	206	114	0.64	72.9	[35]
EM-CCG	1.25	EMIMBF$_4$/AN [3.5 V]	0.1 A g^{-1}	209	261.3	110.3	0.54	59.9	[19]
	1.33	1 M H_2SO_4 [1.0 V]	0.1 A g^{-1}	191.7	255.5	–	–	–	[19]
Compressed-aMEGO	0.75	EMIMBF$_4$/AN [3.5 V]	100 mV s^{-1}	147	110	48	–	–	[61]
VArGO	1.18	6 M KOH [0.7 V]	0.05 A g^{-1}	145	171	7.43	–	–	[53]
HPGM	1.58	6 M KOH [1.0 V]	0.1 A g^{-1}	238	376	13.1	–	–	[46]
		1 M TEMABF$_4$/AN [2.5 V]	0.1 A g^{-1}	108	171	37.1	–	–	[46]
PaGM	0.87	BMIM BF$_4$ [4.0 V]	0.1 A g^{-1}	172.4	150	82.9	0.78	64.7	[69]
Holey graphene film	1.2	EMITFSI [2.5 V]	3 A g^{-1}	45	54	12	–	–	[54]
HGF	0.71	6 M KOH [1.0 V]	1 A g^{-1}	310	221	–	–	–	[76]
	0.71	EMIMBF$_4$/AN [3.5 V]	1 A g^{-1}	298	212	79.4	0.62	49.2	[76]
aPG	0.72	BMIMPF$_6$/AN [3.5 V]	0.5 A g^{-1}	207	149	64			[78]
Graphene/SWNT film	1.06	EMIMBF$_4$ [4.0 V]	0.5 g^{-1}	199	211	117.2	–	–	[55]
PANI/graphene	1.47	1 M H_2SO_4 [0.8 V]	0.1 A g^{-1}	546	802	17.8	–	–	[68]
PANI-CCG gel film	1.25	1 M H_2SO_4 [0.9 V]	5 A g^{-1}	458	572	15.8	–	–	[52]

orderly porous structure with an appropriate gradient to form a dense electrode means that the pore arrangement moves from macropores to micropores at the surface to the internal electrode, which may be a novel approach toward realizing attractive volumetric performance.

The novel 2D TMDs exhibit exceptional cation-intercalation capacitance in a three-electrode system with aqueous electrolyte because of the narrow interlayer spacing, and the cation-intercalation feature is more suitable for the smaller cation intercalation[27] but not for larger anions, restricting its potential application in anode materials and resultant symmetric two-electrode systems. An effective strategy should be introduced to prevent the tight restacking of 2D TMD nanosheets and tune the small interlayer spacing while building a continuous ion transport network for both cations and anions simultaneously, increasing the interfacial contact with the electrolyte and leading to an exceptionally high volumetric capacitance and energy density.

The pursuit of ecofriendly ECs with high volumetric performance involves both electrode material design and device configuration. Since the energy density of ECs is proportional to the capacitance and the square of the voltage, extensive research currently aims at increasing the operating voltage of ECs with organic electrolytes. Unfortunately, organic electrolytes present serious disadvantages, such as low conductivity, a moisture-free atmosphere, and environmentally unfriendly chemicals.[79] Thus, aqueous electrolytes seem to be more acceptable from an industrial point of view in the long term. However, in aqueous media, the operating voltage is usually less than 1.0 V, which limits the energy density of ECs. The use of a highly concentrated aqueous salt electrolyte has been an efficient route to enhance EC performance because this highly concentrated electrolyte can explore the operative voltage of ECs.[80,81] Fabricating a dense yet porous electrode coupled with solvated ions from the highly concentrate aqueous electrolyte ions is a suitable research avenue to promote the development of compact capacitive energy storage.

6. Summary

Here, we have clarified the crucial importance of volumetric performance for the future design and development of ECs. This study provides an in-depth summary of significant research breakthroughs achieved for enhancing the volumetric performance of different dense electrodes in recent years. The emphasis of this review is on discussing the design of densely packed porous carbon electrodes with superior volumetric performance by subtle pore engineering. Furthermore, the

progress of novel 2D metal-inclusive materials such as MXenes and their composites as cation-intercalation electrode materials has also been reviewed at the same time. The ultrahigh cation-intercalation volumetric capacitance of these novel 2D metal-inclusive materials (as negative electrode) indicates a strong potential in compact energy storage systems due to their higher packing density and favorable electrical conductivity. Despite some serious challenges, we firmly believe that pore-engineered electrode materials with higher volumetric performance will be eventually realized in the future.

Acknowledgements

This work was supported by grants from the National Basic Research Program of China (Grant No. 2015CB965000), the National Natural Science Foundation of China (Grant Nos. U1503292 and 21303251), and the Innovation Program of Shanghai Municipal Education Commission (16SG17). The authors also thank Prof. Dan Li and Ke Zhang for discussions.

Conflict of Interest

The authors declare no conflict of interest.

Keywords

capacitive energy storage, dense electrodes, electrolyte ions, pore engineering, volumetric performance

Received: September 30, 2017
Revised: November 3, 2017
Published online:

[1] J. M. Tarascon, M. Armand, *Nature* **2001**, *414*, 359.
[2] P. Simon, Y. Gogotsi, B. Dunn, *Science* **2014**, *343*, 1210.
[3] B. C. Steele, A. Heinzel, *Nature* **2001**, *414*, 345.
[4] C. Zhang, W. Lv, Y. Tao, Q. Yang, *Energy Environ. Sci.* **2015**, *8*, 1390.
[5] Z. Cao, B. Wei, *Energy Environ. Sci.* **2013**, *6*, 3183.
[6] M. Zhao, Q. Zhang, J. Huang, G. Tian, T. Chen, W. Qian, F. Wei, *Carbon* **2013**, *54*, 403.
[7] H. Niu, D. Zhou, X. Yang, X. Li, Q. Wang, F. Qu, *J. Mater. Chem. A* **2015**, *3*, 18413.
[8] Q. Wang, J. Yan, Z. Fan, *Energy Environ. Sci.* **2016**, *9*, 729.
[9] P. Simon, Y. Gogotsi, *Nat. Mater.* **2008**, *7*, 845.
[10] Y. Gogotsi, P. Simon, *Science* **2011**, *334*, 917.
[11] A. Burke, *Electrochim. Acta* **2007**, *53*, 1083.
[12] D. Linden, T. B. Reddy, *Handbook of Batteries*, McGraw-Hill Publishers, NY **2001**.
[13] P. Yang, J. M. Tarascon, *Nat. Mater.* **2012**, *11*, 560.
[14] L. Zhang, F. Zhang, X. Yang, K. Leng, Y. Huang, Y. Chen, *Small* **2013**, *9*, 1342.
[15] V. R. A. Alonso, C. Blanco, R. Santamaria, M. Granda, R. Menedez, S. G. E. de Jager, *Carbon* **2006**, *44*, 441.
[16] T. T. I. Tallo, H. Kurig, K. Kontturi, A. Janes, E. Lust, *Carbon* **2014**, *67*, 607.
[17] Y. Zhou, M. Ghaffari, M. Lin, E. M. Parsons, Y. Liu, B. L. Wardle, Q. M. Zhang, *Electrochim. Acta* **2013**, *111*, 608.
[18] A. B. F. M. Sevilla, *ACS Nano* **2014**, *8*, 5069.
[19] X. Yang, C. Cheng, Y. Wang, L. Qiu, D. Li, *Science* **2013**, *341*, 534.
[20] M. Ghaffari, Y. Zhou, H. Xu, M. Lin, T. Y. Kim, R. S. Ruoff, Q. Zhang, *Adv. Mater.* **2013**, *25*, 4879.
[21] Z. Lei, L. Lu, X. Zhao, *Energy Environ. Sci.* **2012**, *5*, 6391.
[22] Y. Zhou, N. Lachman, M. Ghaffari, H. Xu, D. Bhattacharya, P. Fattahi, M. R. Abidian, S. Wu, K. K. Gleason, B. L. Wardle, Q. Zhang, *J. Mater. Chem. A* **2014**, *2*, 9964.
[23] Q. Wu, Y. Xu, Z. Yao, A. Liu, G. Shi, *ACS Nano* **2010**, *4*, 1963.
[24] M. R. Lukatskaya, O. Mashtalir, C. E. Ren, Y. Dall'Agnese, P. Rozier, P. L. Taberna, M. Naguib, P. Simon, M. W. Barsoum, Y. Gogotsi, *Science* **2013**, *341*, 1502.
[25] M. Ghidiu, M. R. Lukatskaya, M. Zhao, Y. Gogotsi, M. W. Barsoum, *Nature* **2014**, *516*, 78.
[26] M. R. Lukatskaya, S. Kota, Z. Lin, M. Zhao, N. Shpigel, M. D. Levi, J. Halim, P. L. Taberna, M. W. Barsoum, P. Simon, Y. Gogotsi, *Nat. Energy* **2017**, *2*, 17105.
[27] M. Acerce, D. Voiry, M. Chhowalla, *Nat. Nanotechnol.* **2015**, *10*, 313.
[28] D. Kang, Q. Liu, J. Gu, Y. Su, W. Zhang, D. Zhang, *ACS Nano* **2015**, *9*, 11225.
[29] E. Raymundo-Pinero, F. Leroux, F. Beguin, *Adv. Mater.* **2006**, *18*, 1877.
[30] V. Subramanian, C. Luo, A. M. Stephan, K. S. Nahm, S. Thomas, B. Q. Wei, *J. Phys. Chem. C* **2007**, *111*, 7527.
[31] H. Wang, Q. Gao, J. Hu, *J. Am. Chem. Soc.* **2009**, *131*, 7016.
[32] H. Wang, Q. Gao, J. Hu, Z. Chen, *Carbon* **2009**, *47*, 2259.
[33] K. Xia, Q. Gao, C. Wu, S. Song, M. Ruan, *Carbon* **2007**, *45*, 1989.
[34] J. Hu, H. Wang, Q. Gao, H. Guo, *Carbon* **2010**, *48*, 3599.
[35] Y. Bu, T. Sun, Y. Cai, L. Du, O. Zhuo, L. Yang, Q. Wu, X. Wang, Z. Hu, *Adv. Mater.* **2017**, *29*, 1700470.
[36] J. Chmiola, C. Largeot, P. L. Taberna, P. Simon, Y. Gogotsi, *Science* **2010**, *328*, 480.
[37] M. Heon, S. Lofland, J. Applegate, R. Nolte, E. Cortes, J. D. Hettinger, P. L. Taberna, P. Simon, P. H. Huang, M. Brunet, Y. Gogotsi, *Energy Environ. Sci.* **2011**, *4*, 135.
[38] J. Chmiola, G. Yushin, R. Dash, Y. Gogotsi, *J. Power Sources* **2006**, *158*, 765.
[39] J. Yan, Q. Wang, C. Lin, T. Wei, Z. Fan, *Adv. Energy Mater.* **2014**, *4*, 1400500.
[40] P. Simon, Y. Gogotsi, *Nat. Mater.* **2008**, *7*, 845.
[41] P. Simon, Y. Gogotsi, *Acc. Chem. Res.* **2013**, *46*, 1094.
[42] D. N. Futaba, K. Hata, T. Yamada, T. Hiraoka, Y. Hayamizu, Y. Kakudate, O. Tanaike, H. Hatori, M. Yumura, S. Iijima, *Nat. Mater.* **2006**, *5*, 987.
[43] S. W. Lee, B. S. Kim, S. Chen, Y. Shao-Horn, P. T. Hammond, *J. Am. Chem. Soc.* **2009**, *131*, 671.
[44] Y. Zhu, S. Murali, M. D. Stoller, K. J. Ganesh, W. Cai, P. J. Ferreira, A. Pirkle, R. M. Wallace, K. A. Cychosz, M. Thommes, D. Su, E. A. Stach, R. S. Ruoff, *Science* **2011**, *332*, 1537.
[45] B. Mendoza-Sanchez, Y. Gogotsi, *Adv. Mater.* **2016**, *28*, 6104.
[46] Y. Tao, X. Xie, W. Lv, D. Tang, D. Kong, Z. Huang, H. Nishihara, T. Ishii, B. Li, D. Golberg, F. Kang, T. Kyotani, Q. Yang, *Sci. Rep.* **2013**, *3*, 2975.
[47] K. S. W. Sing, D. H. Everett, R. A. W. Haul, L. Moscou, R. A. Pierotti, J. Rouquerol, T. Siemieniewska, *Pure Appl. Chem.* **1985**, *57*, 603.
[48] A. G. Pandolfo, A. F. Hollenkamp, *J. Power Sources* **2006**, *157*, 11.
[49] D. Wang, F. Li, M. Liu, G. Lu, H. Cheng, *Angew. Chem., Int. Ed.* **2008**, *47*, 373.
[50] C. Lin, J. A. Ritter, B. N. Popov, *J. Electrochem. Soc.* **1999**, *146*, 3639.
[51] C. Largeot, C. Portet, J. Chmiola, P. L. Taberna, Y. Gogotsi, P. Simon, *J. Am. Chem. Soc.* **2008**, *130*, 2730.
[52] Y. Wang, X. Yang, A. G. Pandolfo, J. Ding, D. Li, *Adv. Energy Mater.* **2016**, *6*, 1600185.
[53] Y. Yoon, K. Lee, S. Kwon, S. Seo, H. Yoo, S. Kim, Y. Shin, Y. Park, D. Kim, J. Y. Choi, H. Lee, *ACS Nano* **2014**, *8*, 4580.

[54] X. Han, M. R. Funk, F. Shen, Y. Chen, Y. Li, C. J. Campbell, J. Dai, X. Yang, J. W. Kim, Y. Liao, J. W. Connell, V. Barone, Z. Chen, Y. Lin, L. Hu, *ACS Nano* **2014**, *8*, 8255.
[55] D. T. Pham, T. H. Lee, D. H. Luong, F. Yao, A. Ghosh, V. T. Le, T. H. Kim, B. Li, J. Chang, Y. H. Lee, *ACS Nano* **2015**, *9*, 2018.
[56] J. Chmiola, G. Yushin, Y. Gogotsi, C. Portet, P. Simon, P. L. Taberna, *Science* **2006**, *313*, 1760.
[57] C. Prehal, C. Koczwara, N. Jäckel, A. Schreiber, M. Burian, H. Amenitsch, M. A. Hartmann, V. Presser, O. Paris, *Nat. Energy* **2017**, *2*, 16215.
[58] N. Jäckel, P. Simon, Y. Gogotsi, V. Presser, *ACS Energy Lett.* **2016**, *1*, 1262.
[59] W. Y. Tsai, P. L. Taberna, P. Simon, *J. Am. Chem. Soc.* **2014**, *136*, 8722.
[60] E. Mourad, L. Coustan, P. Lannelongue, D. Zigah, A. Mehdi, A. Vioux, S. A. Freunberger, F. Favier, O. Fontaine, *Nat. Mater.* **2017**, *16*, 446.
[61] S. Murali, N. Quarles, L. Zhang, J. R. Potts, Z. Tan, Y. Lu, Y. Zhu, R. S. Ruoff, *Nano Energy* **2013**, *2*, 764.
[62] A. Izadi-Najafabadi, S. Yasuda, K. Kobashi, T. Yamada, D. N. Futaba, H. Hatori, M. Yumura, S. Iijima, K. Hata, *Adv. Mater.* **2010**, *22*, E235.
[63] K. Xie, X. Qin, X. Wang, Y. Wang, H. Tao, Q. Wu, L. Yang, Z. Hu, *Adv. Mater.* **2012**, *24*, 347.
[64] Z. Y. Lyu, D. Xu, L. Yang, R. Che, R. Feng, J. Zhao, Y. Li, Q. Wu, X. Wang, Z. Hu, *Nano Energy* **2015**, *12*, 657.
[65] N. A. Kumar, H. J. Choi, Y. R. Shin, D. W. Chang, L. Dai, J. B. Baek, *ACS Nano* **2012**, *6*, 1715.
[66] Y. Wang, X. Yang, L. Qiu, D. Li, *Energy Environ. Sci.* **2013**, *6*, 477.
[67] P. Yu, X. Zhao, Z. Huang, Y. Li, Q. Zhang, *J. Mater. Chem. A* **2014**, *2*, 14413.
[68] Y. Xu, Y. Tao, X. Zheng, H. Ma, J. Luo, F. Kang, Q. H. Yang, *Adv. Mater.* **2015**, *27*, 8082.
[69] H. Li, Y. Taoa, X. Zheng, J. Luo, F. Kang, H. Cheng, Q. Yang, *Energy Environ. Sci.* **2016**, *9*, 3135.
[70] M. Naguib, M. Kurtoglu, V. Presser, J. Lu, J. Niu, M. Heon, L. Hultman, Y. Gogotsi, M. W. Barsoum, *Adv. Mater.* **2011**, *23*, 4248.
[71] J. Yan, C. Ren, K. Maleski, C. B. Hatter, B. Anasori, P. Urbankowski, A. Sarycheva, Y. Gogotsi, *Adv. Funct. Mater.* **2017**, *27*, 1701264.
[72] M. Boota, B. Anasori, C. Voigt, M. Zhao, M. W. Barsoum, Y. Gogotsi, *Adv. Mater.* **2016**, *28*, 1517.
[73] Y. Lin, K. A. Watson, J. W. Kim, D. W. Baggett, D. C. Working, J. W. Connell, *Nanoscale* **2013**, *5*, 7814.
[74] Z. Bo, W. Zhu, W. Ma, Z. Wen, X. Shuai, J. Chen, J. Yan, Z. Wang, K. Cen, X. Feng, *Adv. Mater.* **2013**, *25*, 5799.
[75] X. Yang, J. Zhu, L. Qiu, D. Li, *Adv. Mater.* **2011**, *23*, 2833.
[76] Y. Xu, Z. Lin, X. Zhong, X. Huang, N. O. Weiss, Y. Huang, X. Duan, *Nat. Commun.* **2014**, *5*, 4554.
[77] G. Hao, A. Lu, W. Dong, Z. Jin, X. Zhang, J. Zhang, W. Li, *Adv. Energy Mater.* **2013**, *3*, 1421.
[78] J. Xu, Z. Tan, W. Zeng, G. Chen, S. Wu, Y. Zhao, K. Ni, Z. Tao, M. Ikram, H. Ji, Y. Zhu, *Adv. Mater.* **2016**, *28*, 5222.
[79] F. Beguin, V. Presser, A. Balducci, E. Frackowiak, *Adv. Mater.* **2014**, *26*, 2219.
[80] L. Suo, O. Borodin, T. Gao, M. Olguin, J. Ho, X. Fan, C. Luo, C. Wang, K. Xu, *Science* **2015**, *350*, 938.
[81] Y. Yamada, K. Usui, K. Sodeyama, S. Ko, Y. Tateyama, A. Yamada, *Nat. Energy* **2016**, *1*, 16129.